17th World Conference on Earthquake Engineering, 17WCEE
Sendai, Japan - September 13th to 18th 2020

EFFECTS OF MEMBER CONFIGURATIONS ON SHEAR CAPACITIES OF BEAM-COLUMN JOINTS CONSTRUCTED BY "RCST" COMPOSITE SYSTEM

K. Sawaguchi [1], D. Ishii [2], K. Yamanobe[3] , K. Ogura[4] , T. Nishiya[5]

[1] *Research Engineer, Shimizu Corporation, kaori_okubo@shimz.co.jp*
[2] *Senior Research Engineer, Shimizu Corporation, daigo_ishii@shimz.co.jp*
[3] *Chief Research Engineer, Shimizu Corporation, yamanobe@shimz.co.jp*
[4] *Manager, Shimizu Corporation, k.ogura@shimz.co.jp*
[5] *Chief design group manager, Shimizu Corporation, t.nishiya@shimz.co.jp*

Abstract

In order to improve building construction productivities, the authors developed a composite frame system called RCST (Reinforced Concrete Steel Tube) system that has been utilized for more than 20 years. The RCST system consists of concrete-filled steel-tube columns, H-shaped steel beams and beam-column joints with steel cover plates for confinement. Column steel tubes are not welded to the beam-column joint, which leads to the rapid erection of the upper column on the floor. Columns and beam-column joints are easily connected by casting concrete and by the connecting rebars arranged through the upper/lower columns and the beam-column joints. The system has been mainly applied to mid or low-rise buildings such as logistics and commercial facilities so far.

In response to growing demand for large-scale RCST buildings, the authors have performed several series of experiments in order to extend the range of application and to update the conventional RCST design method with sufficient data for a design review. This paper describes one of the static loading tests to investigate the effect of member configurations, for instance the column-to-beam depth and the width ratios, on joint shear capacities. Four RCST inner beam-column joint specimens of 1/2 scale were tested under static reversal loadings and a constant axial load. While the conventional column-to-beam depth ratio D_c/D_b shall be between 1.4 and 4.0, and the width ratio B_c/B_b between 2.6 and 5.0, each specimen in this project was designed so as to fail in its joint, with D_c/D_b of 1.0~1.4 and with B_c/B_b of 2.6~4.0.

The maximum shear strengths of specimen No.1 and No.2 (D_c/D_b of 1.4, B_c/B_b of 2.6) were larger than the calculated ones by 4～10%, on the other hand, those of specimen No.3(D_c/D_b of 1.4, B_c/B_b of 4.0) and No.4 (D_c/D_b of 1.0, B_c/B_b of 4.0) were smaller. Since the drift angle due to the joint of each specimen increased after the maximum peak load, it confirmed that each specimen failed in its joint. Based on the investigation on the stress distribution of joint elements and the existing empirical data in terms of the member configurations and the joint-to-beam strength ratio, the authors suggested the conventional design method should be modified to evaluate shear capacities of RCST beam-column joints.

Keywords: composite frame system; concrete-filled steel-tube; static loading test; member configurations

1. Introduction

The RCST (Reinforced Concrete Steel Tube) frame is a composite structural system which has been in use for over 20 years to improve building construction productivities [1]. As shown in Fig. 1, it consists of concrete-filled steel-tube columns, H-shaped steel beams and beam-column joints of steel cover plates for confinement. Both the top and bottom of column steel-tubes are not welded to beam-column joints, leading to the rapid erection of the upper column on the floor. Columns and beam-column joints are easily connected by casting concrete and by the connecting rebars arranged through the upper/lower columns and the beam-column joints. Thus, RCST structures are designed in accordance with the R/C design code for column ends, the steel design code for steel beams, and the conventional RCST design method for joints and column shafts. The RCST design method for joints refers to another composite system called RCSS (Reinforced-Concrete & Steel System) [2][3][4].

Recently, the demand for large-scale RCST buildings is growing. The authors have performed several series of experiments in order to extend the application scope and to update the conventional RCST design method for a design review. This paper describes the outline and the results of a static loading experiment in order to investigate the effect of member configurations on joint shear capacities.

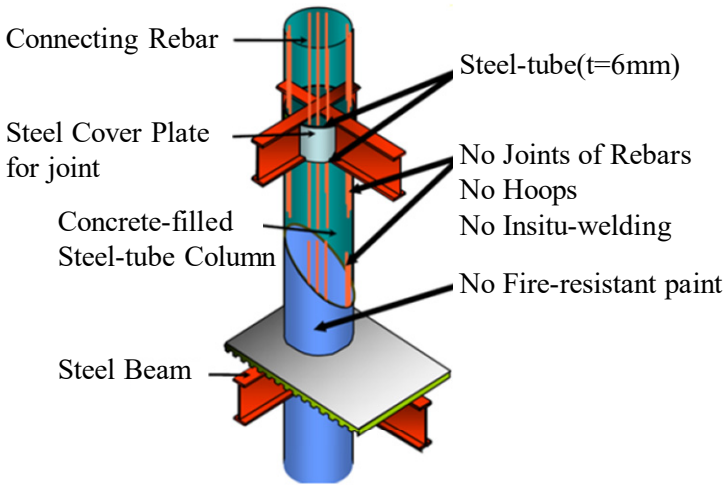

Fig. 1 – RCST composite structural system

2. Experiment Outline

2.1 Specimen

Four half-scale RCST interior beam-column joint specimens were tested in 2018. They were designed to first fail in a joint based on the allowable stress design method for RCST structures. The beam and column geometries were chosen from a mid-rise model building, with a grid span of from 9 to 12 m and, the column height of from 3 to 3.9 m. The typical column diameter is from 800 to 900 mm.

Table 1 shows the parameters of each specimen. The parameters are (a) column-to-beam depth ratio (D_c/D_b), (b) column-to-beam width ratio (B_c/B_b), and (c) design strength of concrete. The column steel-pipe and the joint steel cover plate were of PL3.2(SS400) and with 450 mm in diameter. As shown in Fig. 2, the specimen beam span was 4.4 m and the column height was 2.7 m. The connecting rebars were arranged with the concrete coverage to the column steel-pipe of 15 mm, and to the beam-flange rim of 5 mm. SN490B was used for beam-flanges and webs in all specimens.

Figure 3 compares the detail of specimens. Specimens No. 1 and No. 2 had the same depth ratio D_c/D_b of 1.4 and width ratio B_c/B_b of 2.6, using concrete with the design compressive strength of 30 MPa and 60 MPa, respectively. The cross-section of the beams was 320 x 170 x 9 x 32 and 320 x 170 x 9 x 36 mm, for specimens No. 1 and No. 2, respectively. Specimen No. 3, with B_c/B_b of 4.0, had the same D_c/D_b (1.4) and concrete design strength (60 MPa) as specimen No. 2. The cross-section of the specimen No.3 beams was 320 x 110 x 9 x 40 mm. Specimen No. 4, with D_c/D_b of 1.0, had the same B_c/B_b of 4.0 and concrete design strength of 60 MPa as specimen No. 3. The cross-section of the specimen No.4 beams was 450 x 110 x 9 x 32 mm. Twelve D19 bars were arranged for the connecting reinforcement with adequate design development length according to the concrete design strength. To ensure the joint failure, the beam-web thickness in the joint was thinner than the outside. The web thicknesses were 4.5 mm for specimens No. 1 and No. 2, and 3.0 mm for specimens No. 3 and No. 4, respectively.

Table 1 –Parameters of test specimens

Specimen	Geometry		Concrete	Column				Beam*
	Dc/Db	Bc/Bb		Axial Load (kN)	Dc (mm)	Rebar	Development Length (mm)	
No. 1	1.41	2.65	Fc30	1980	450	12-D19 (SD490)	990	BH-320 x 170 x 9 x 32
No. 2	1.41	2.65	Fc60	2900			745	BH-320 x 170 x 9 x 36
No. 3	1.41	4.09	Fc60					BH-320 x 110 x 9 x 40
No. 4	1.00	4.09	Fc60					BH-450 x 110 x 9 x 32

*The web thickness in the joint; 4.5mm for specimens No. 1 and No. 2, 3.0mm for specimens No. 3 and No. 4

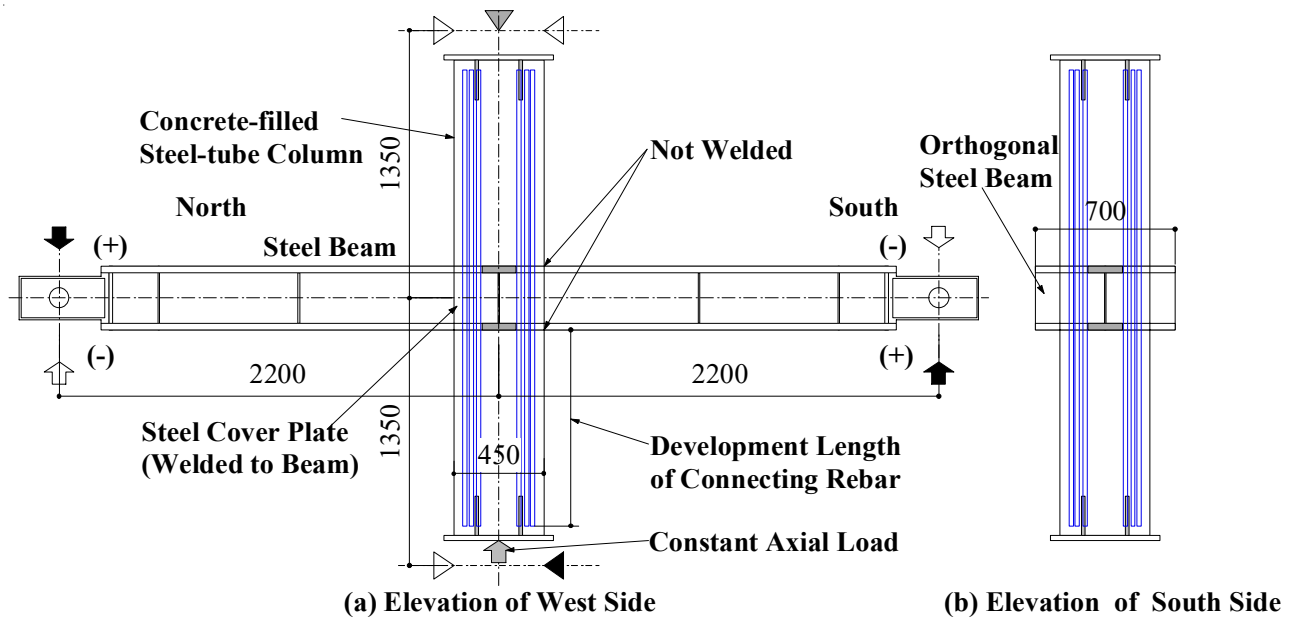

Fig. 2 – Geometry and detail of test specimens

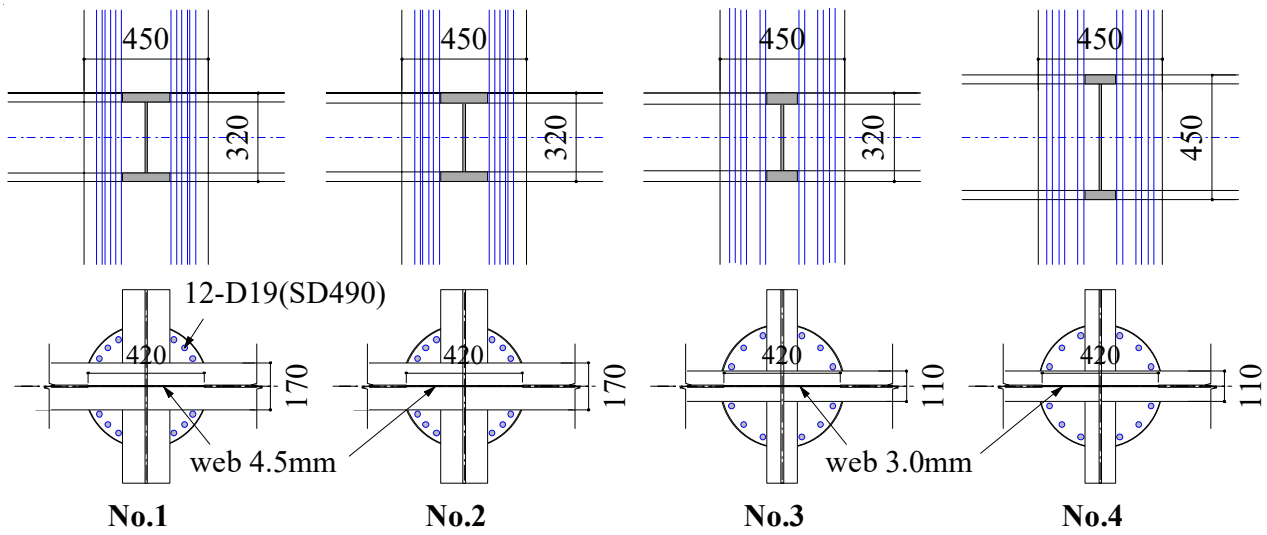

Fig. 3 – Comparison of beam-column joints in test specimens

Table 2 – Mechanical properties of concrete

Specimen	Compressive strength (MPa)	Tensile strength (MPa)	Young's modulus (GPa)	Poisson's ratio
No. 1	42.7	3.26	29.3	0.20
No. 2	77.6	3.63	34.5	0.21
No. 3	77.6	3.63	34.5	0.21
No. 4	78.9	3.77	35.6	0.22

Table 3 – Mechanical properties of steel

Type	Thickness (mm)	Yield point (MPa)	Tensile strength (MPa)	Young's modulus (GPa)
PL3 SN490B	3	366	557	208
PL4.5 SN490B	4.5	356	555	207
PL9 SN490B	9	354	558	210
PL32 SN490B	32	337	529	211
PL36 SN490B	36	359	532	213
PL40 SN490B	40	342	529	208
PL3.2 SS400	3.2	370	473	209
D19 SD490	ϕ =19	522	696	190

2.2 Materials

The mechanical properties of the concrete and the steel are shown in Table 2 and Table 3. Concrete was of normal Portland cement with a normal density with the nominal maximum aggregate size of 13mm. The average compressive strengths of the concrete obtained by the cylinder tests were 42.7 MPa, 77.6 MPa, 78.9 MPa, for specimens No. 1, No. 2 and No. 3, and No. 4, respectively. The steel beam was of SN490B, and the column steel tube and the steel cover plate for joints were of SS400. SD490 was used for the connecting rebars.

2.3 Test program

Figure 4 shows the loading setup. The specimens were supported by a roller at the column bottom and a pin at the top. The static cyclic loads were applied to the beam ends with the two 1MN capacity hydraulic jacks in order to exert an antisymmetric moment distribution in the specimen. A constant axial load was applied to the column with a 3 MN capacity hydraulic jack at the bottom.

The loading history is shown in Table 4. The story drift angle R is defined as the relative vertical displacement of the beams in the column coordinate divided by the beam span of 4.4 m. The story drift angles were imposed ranging from ±0.125% to +5.0%. Two cycles of the same story drift angle were repeated from ±0.25% to ±2.0%. The axial load for specimen No.1 was 1980 kN corresponding to the axial force ratio of 0.3. The axial load of 2900 kN corresponding to the axial force ratio of 0.24 was applied for specimens No. 2, No. 3 and No. 4.

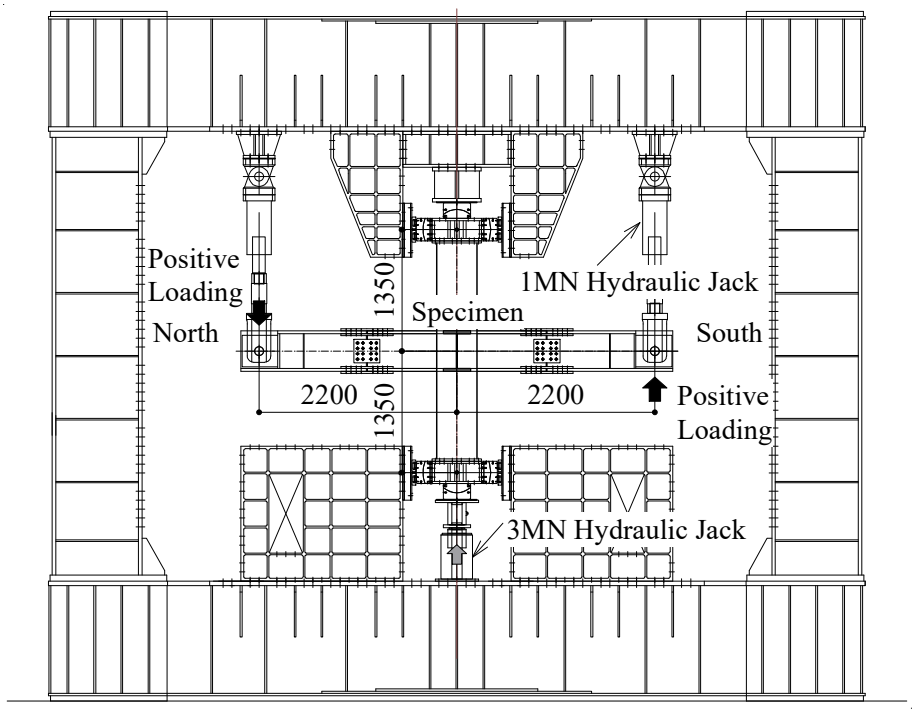

Fig. 4 – Loading system (Elevation of West side)

Table 4 – Loading history of story drift angle

Cycle number	**1**	**2-3**	**4-5**	**6-7**	**8-9**	**10-11**	**12**	**13**
Story drift angle (%)	±0.125	±0.25	±0.50	±1.0	±1.5	±2.0	±3.0	+5.0

3. Test Results

3.1 Damage configuration

Figure 5 shows the cracking patterns of the joint concrete inside the steel cover plate after loading. Each crack was emphasized by marker ink. Several horizontal cracks from the principal beam-flange and some vertical cracks along the orthogonal beam-web were observed in all specimens. In addition, the diagonal cracks from the upper/lower orthogonal beam flange to the lower/upper principal beam flange were wider than the horizontal and vertical ones.

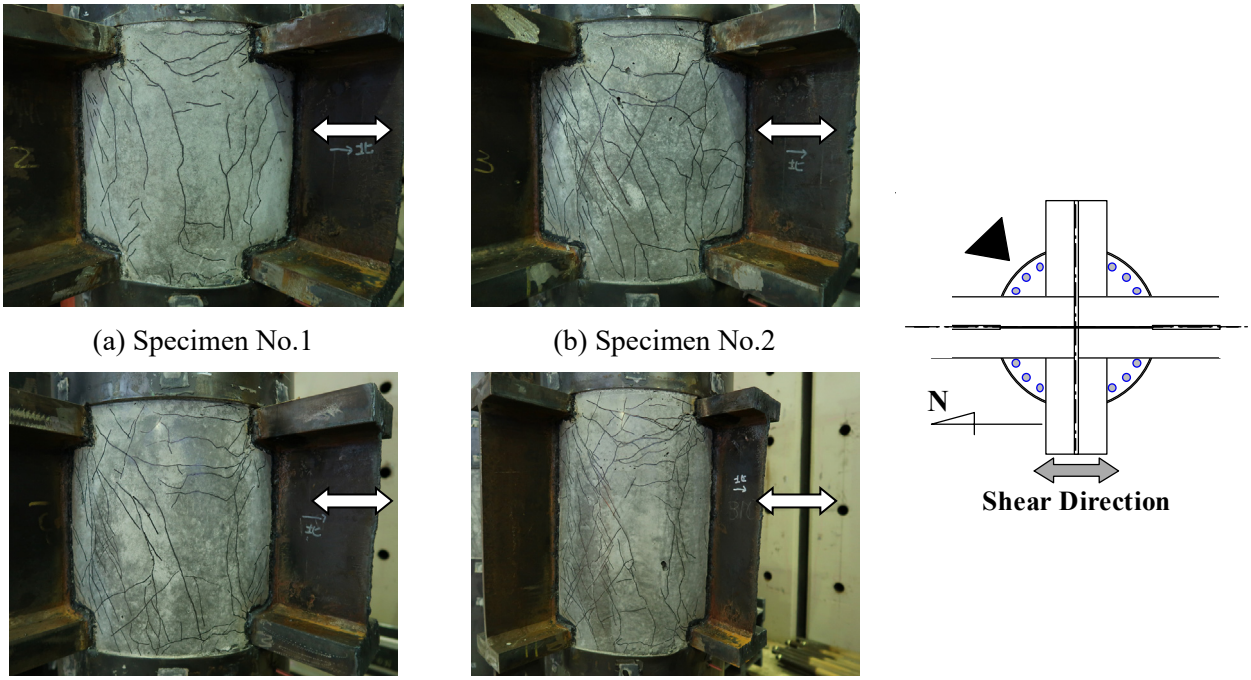

(a) Specimen No.1 (b) Specimen No.2

(c) Specimen No.3 (d) Specimen No.4

Fig. 5 – Cracking patterns of joint concrete after loading (North-East side)

3.2 Summary of test results

The test results were summarized in Table 5. In all specimens, the joint cover steel plates yielded at the story drift angle of around 0.5%. The yielding of beam-web was observed at the story drift angle of -0.30%, -0.42%, 0.49%, 0.48% for specimens No. 1, No. 2, No. 3 and No. 4, respectively. As for specimens No. 3 and No. 4, the beam-flange yielded before the story shear reached the calculated story shear at joint failure. Therefore, specimens No. 1 and No. 2 failed in the joint, while specimens No. 3 and No. 4 in beam-flexure. This indicated that the beam flexural failure occurred unexpectedly because the concrete compressive strengths of specimens No. 3 and No. 4 were much higher than the design strength of 60 MPa.

The maximum story shear of specimen No. 1 with the width ratio B_c/B_b of 2.6, was larger than the calculated story shear at joint failure in the positive loading direction, but lower in the negative loading direction. On the other hand, specimen No. 2 with B_c/B_b of 2.6 had larger story shear than the calculated joint strength in both directions by 4~8%. As for specimens No. 3 and No. 4 with B_c/B_b of 4.0, the maximum story shear was smaller than the calculated joint strength by 1~6%.

Table 5 – Summary of test results

Specimen		No. 1	No. 2	No. 3	No. 4
Story shear (kN)	Maximum (+)	341.3	437.9	380.8	470.2
	Minimum (-)	-327.7	-422.7	-377.6	-455.5
	of joint shear strength	327.6	398.9	382.4	479.2
Maximum shear (+) / joint strength ratio		1.04	1.10	0.996	0.981
Story drift angle (%)	Maximum (+)	4.97	3.03	3.03	3.02
	Minimum (-)	-3.01	-3.01	-3.04	-2.00
Failure mode*		J	J	BJ	B
Story shear at yielding (kN)	of steel cover plate	126.9	-142.9	137.7	146.1
	of beam-web in joint	-106.2	-158.9	136.9	209.2
	of beam-flange	—	—	-297.8	349.7
Story drift angle at yielding (%)	of steel cover plate	0.44	-0.38	0.50	0.37
	of beam-web in joint	-0.30	-0.42	0.49	0.48
	of beam-flange	—	—	-1.33	1.04

*Symbol designates: J: Joint shear failure, B: Beam flexural yield failure, BJ: Beam-flexure followed by joint failure

4. Discussion

4.1 Story shear vs. story drift angle relation

Story shear vs. story drift angle relations are compared in Fig. 6. In the positive loading direction, specimen No. 1 reached the maximum story shear at the cycle of 5% story drift angle, while specimens No. 2, No. 3 and No. 4 reached it at the first cycle of 3%. In the negative loading direction, specimens No. 1, No. 2 and No. 3 reached the maximum story drift shear at the cycle of 3% story drift angle, while specimen No. 4 reached it at the first cycle of 2%. All specimens except specimen No.1 showed a slight degradation of story shear after the cycle of 3% story drift angle, while the loops were stable after joint or beam- flexural failure.

4.2 Effect of the joint-to-beam strength ratio

Figure 7 shows the effect of the joint-to-beam ultimate strength ratio against the ratio of the maximum story shear to the joint shear strength. The data include other existing test results performed in 2017 and 2018. The maximum joint shears of specimens with the joint shear-to-beam flexural strength ratio Q_{ju}/Q_{bu} of less than 0.75 were larger than the joint shear ultimate strength, which means the maximum shear-to-joint shear strength ratios were larger than 1.0. On the other hand, in specimens No. 3 and No. 4 with Q_{ju}/Q_{bu} of about 1.0, the maximum story shear was under the joint shear ultimate strength.

4.3 Joint shear deformation

The story drift angle due to joint shear deformation calculated by the measurement at the end of the beam-web is shown against story drift angle in Fig. 8. The story drift angle due to joint deformation increased

slightly after the story drift angle reached 3%. At the story drift of 5%, specimen No. 3 with the depth ratio D_c/D_b of 1.4 and the width ratio B_c/B_b of 4.0 was the largest, while specimen No. 2 with D_c/D_b of 1.4 and B_c/B_b of 2.6 was the second largest. This indicated that specimen No. 3 yielded in the joint after the beam failed in flexure.

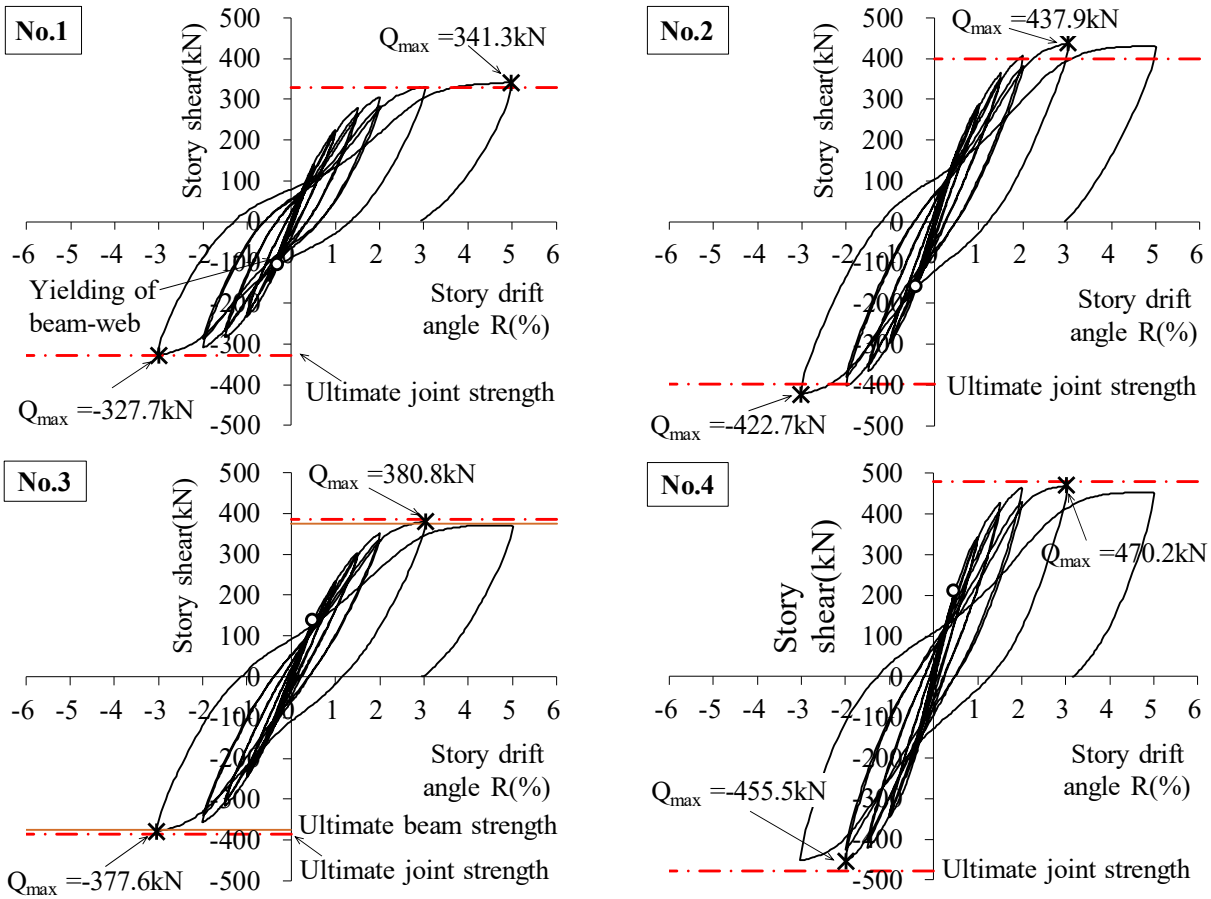

Fig. 6 – Story shear vs. story drift angle relation

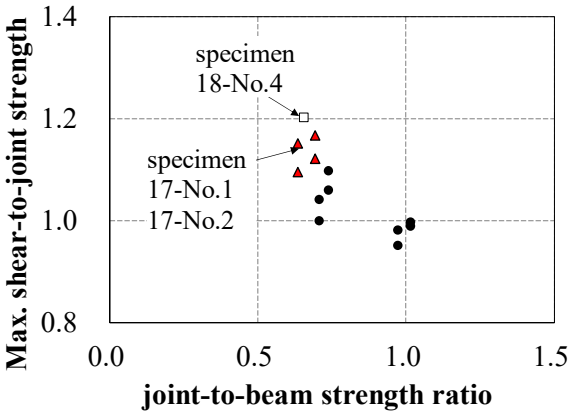

Fig. 7 – Effect of the joint-to-beam strength ratio

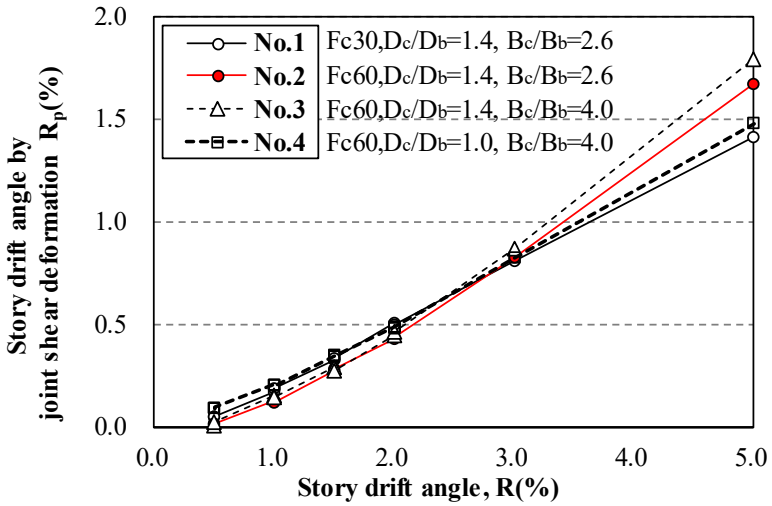

Fig. 8 – Story drift angle due to joint shear deformation

4.4 Joint shear design method

The RCST joint shear design strength Q_p is calculated by Eq.(1). It is assumed that the joint resists through three components: beam-web, steel cover plate, and filled-concrete in steel cover plate.

$$Q_p = Q_w + Q_f + Q_c \tag{1}$$

where, Q_w: the joint shear allowable strength exerted by beam-web, Q_f: the joint shear allowable strength exerted by steel cover plate, and Q_c: the joint shear allowable strength exerted by filled-concrete.

The shear strength components are calculated by Eq.(2) ~Eq.(4), respectively. Each equation consists of the effectiveness factor, the normal shear stress and the effective shear cross-section area.

$$Q_w = k_w \cdot \tau_w \cdot t_w \cdot d \tag{2}$$

$$Q_f = k_f \cdot \tau_f \cdot 0.5A_f \tag{3}$$

$$Q_c = k_c \cdot \tau_c \cdot A_c \tag{4}$$

where, k_w, k_f, k_w: the effectiveness factor, τ_w, τ_f, τ_c: the normal shear strength, t_w: the thickness of beam-web in joint, d: the effective shear depth, A_f: the cross-sectional area of steel cover plate ($=1/4\pi(D_c^2-D_{con}^2)$), and A_c: the cross-sectional area of filled-concrete ($=1/4\pi D_{con}^2$). Figure 9 shows the joint dimensions of the RCST system.

The effectiveness factors, k_w, k_f and k_c, were used to consider the fact that the strains of the steel cover plate and concrete were smaller than that of the beam-web. The factors shown in Table 6 were defined in the previous test results. The normal shear stresses were defined according to the allowable stress design method, shown in Table 7. As for the normal shear stress of concrete τ_c considers the depth ratio D_c/D_b and the material properties of the beam-web. The effective shear cross-sectional areas were due to the joint geometry. The effective shear depth of beam-web, d, is the distance from the compression rim of the filled-concrete to the centroid of tensile connecting rebars. The effective cross-sectional area of steel cover plate is one half of the column steel-pipe cross-sectional area.

Table 6– Effectiveness factor in allowable stress method

Factor	Long-term	Short-term	Ultimate
k_w	1.0	1.0	1.0
k_f	$1.983-0.325D_c/B_b \leqq 0.65$		1.0
k_c	$1.370-0.139D_c/B_b \leqq 0.8$		

Table 7 – Normal shear stress in allowable stress method

Factor	Long-term	Short-term	Ultimate
τ_w	$1.36 \cdot {}_jFs_L^* \cdot {}_j\beta \cdot G_w/G_c$	$F_w/(1.5\sqrt{3})$	$1.1F_w/(\sqrt{3})$
τ_f	$1.36 \cdot {}_jFs_L \cdot {}_j\beta \cdot G_f/G_c$	$F_w/(1.5\sqrt{3})$	$1.1F_f/(\sqrt{3})$
τ_c	$1.36 \cdot {}_jFs_L \cdot {}_j\beta$	$1.36 \cdot \alpha \cdot {}_jFs_L \cdot {}_j\beta$	$1.36 \cdot {}_jFs_u^{**} \cdot {}_j\beta$

* ${}_jFs_L = 2 \cdot (\min(Fc/30, 5+Fc/100))$

** ${}_jFs_u = \min(0.12Fc', 18+3.6 \cdot Fc'/100)$, where $Fc'=Fc+4 \cdot 0.3 \cdot (t_f/r) \cdot s\sigma_y$, $r=(D_c-t_f)/2$, $s\sigma_y=1.1 \cdot F_f$

Where, Fc: the concrete design strength, ${}_j\beta$: $2 \cdot (Dc/Db) \leqq 4.0$, α: 1.23 for SS400 & 1.31 for SM490, F_w & F_f: the normal strength, G_w & G_f: the shear elastic rigidity, t_f: the thickness of steel cover plate, d_t: the distance to rebar-center from the rim of filled-concrete.

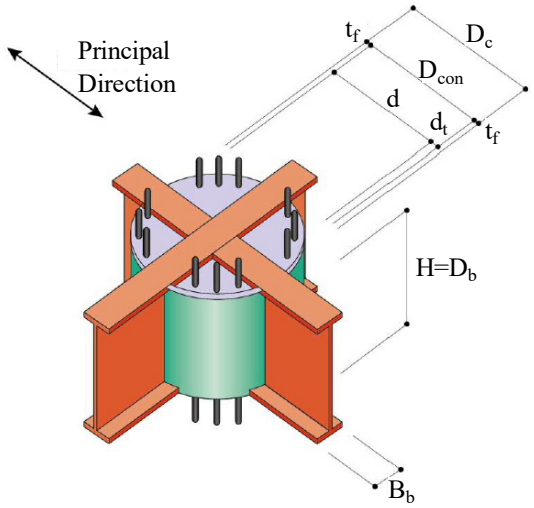

Fig. 9 – Joint dimensions of RCST system

Table 8 shows the calculated effectiveness factors at the story drift angle of 2% by using the test results and the normal shear stresses in the conventional RCST design method. The joint shear forces of beam-web Q_w and steel cover plate Q_f, were calculated by the measured strain data, thus, the shear force of filled-concrete Q_c was equal to the subtraction of the calculated Q_w and Q_f from the experimental joint shear force Q_p. It must be noted that at the story drift angle of 2% all specimens except No.2 did not reached the calculated joint shear strength. The story shear forces of specimens No. 1, No. 3, and No. 4 were 93 %, 92 %, and 97 % of the joint shear strength respectively. The beam-web factor k_w was smaller than the design value of 1.0 in specimens No. 2, No. 3 and No. 4 by 7 % ~ 17 %. For specimens No. 1 and No. 4, the steel cover plate factor k_f was larger than the design value of 1.0, while for specimens No. 2 and No. 3 smaller. As for the filled-concrete factor k_c, it was smaller than the design value of 0.8 in specimens No. 1, No. 3 and No. 4.

Table 8 – Calculated effectiveness factors by the experiment with design normal shear stress

Specimen		No. 1	No. 2	No. 3	No. 4
Member configuration	**Depth ratio D_c/D_b**	1.41	1.41	1.41	1.00
	Width ratio B_c/B_b	2.65	2.65	4.09	4.09
Maximum (+)	**Story shear, Q_c (kN)**	341	438	381	470
	Joint shear, Q_p (kN)	2613	3406	2985	2314
	Story drift angle, R (%)	4.97	3.03	3.03	3.02
Joint shear force, Q_p(kN)	**Observed at R=2% (+)**	2332	3155	2748	2279
	Observed at R=3% (+)	2531	3406	2985	2314
	Calculated (ultimate)	2508	3103	2998	2359
Observed/calculated joint shear force	**at R=2% (+)**	0.93	1.02	0.92	0.97
	at R=3% (+)	1.01	1.10	1.00	0.98
Effectiveness factor for beam-web, k_w (=1.0 in design) At R=2%	**Thickness, t_w (mm)**	4.5		3.0	
	Normal strength, τ_w (MPa)	206		211	
	Observed Strength, Q_w (kN)	362	336	228	212
	Experimental k_w	1.003	0.929	0.889	0.828
	Design / experiment k_w	0.997	1.076	1.124	1.208
Effectiveness factor for steel cover plate, k_f (=1.0 in design) At R=2%	**Number of plate, n_f**	2			
	Thickness, t_f (mm)	3.2			
	Normal strength, τ_f (MPa)	213			
	Observed Strength, Q_f (kN)	527	458	382	500
	Experimental k_f	1.103	0.958	0.799	1.044
	Design / experiment k_f	0.907	1.044	1.252	0.958
Effectiveness factor for filled-concrete, k_c (=0.8 in design) At R=2%	**Concrete strength, σ_B (MPa)**	42.7	77.6	77.6	78.9
	$_jFs_u$ (MPa)	3.53	4.78	4.78	4.82
	$_j\beta$	2.81	2.81	2.81	2.00
	Normal strength, τ_c (MPa)	13.5	18.3	18.3	13.1
	Calculated Strength, Q_c (kN)*	1442	2361	2137	1567
	Experimental k_c	0.692	0.835	0.756	0.773
	Design / experiment k_c	1.156	0.958	1.058	1.035

* Joint shear force by concrete $Q_c = Q_p - (Q_w + Q_f)$, where Q_p: calculated joint shear ultimate strength

Figure 10 shows the relation of the normal shear stress of the filled-concrete τ_c obtained by the observed Q_c and the effectiveness factor k_c in design. The data include the existing test results in 2017, with D_c x B_c, D_b x B_b of 450 x 450, 450 x 170 mm, respectively. Fig. 10 (a) plots the calculated τ_c against the joint aspect ratio indicating factor ${}_j\beta$ (=2 ・ D_c/D_b) in order to investigate the effect of the joint geometry, while Fig. 10 (b) plots against a new proposed factor ${}_j\eta$ (=B_b ・ D_b/(450 x 170)), which stands for the concrete volume between the beam-flanges, to discuss the effect on the concrete-strut force transfer system. None of the factors reasonably explained the difference between the calculated and the design τ_c, especially at ${}_j\beta$ of 2.0 and at ${}_j\eta$ of 1.0. In the 2018 results, the obtained τ_c showed a positive correlation in both ${}_j\beta$ and ${}_j\eta$.

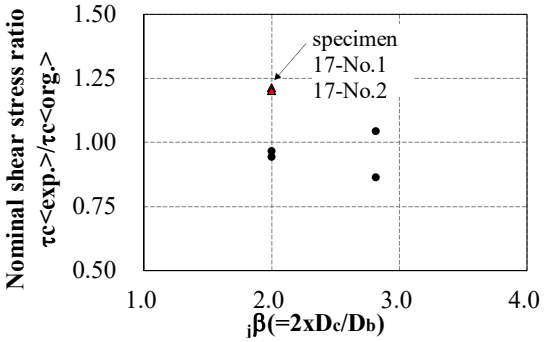

(a) Effect of factor ${}_j\beta$

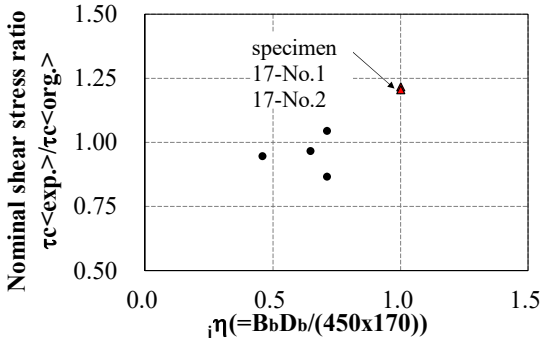

(b) Effect of concrete volume among beam-flanges

Fig. 10 – Relation of the obtained normal stress of concrete τ_c against ${}_j\beta$ and ${}_j\eta$

5. Conclusion

A static loading test of RCST interior beam-column joints was carried out in order to investigate the effect of the column-to-beam depth and width ratios. The test results indicated that (1) the maximum story shear forces of specimens with the width ratio of 2.6 reached the calculated ultimate joint shear strength, but specimens with the width ratio of 4.0 showed the lower strength, (2) the conventional RCST design factor for joint shear strength overestimated the shear capacities of joint components; about 8~21% larger in beam-web; 4~25 % larger in steel cover plate, (3) both of the normal concrete shear stress τ_c calculated by the observed shear forces and the design factor k_c had a positive correlation with the depth ratio and the volume of confined concrete between beam-flanges. Further studies would contribute to modify the design method for RCST joint shear strength.

6. References

[1] Nakagawa K, Architectural Institute of Japan (1999): Development of RCST structural system part 1 outline of structural system & experimental results. *Summaries of technical papers of annual meeting*, 1047-1048. (in Japanese)

[2] Sakaguchi N, Architectural Institute of Japan (1991): Shear capacity of beam-column connection between steel beams and reinforced concrete columns. *Journal of Structure and Construction Engineering*, **428**, 69-78. (in Japanese)

[3] Sakaguchi N, Architectural Institute of Japan (1991): Shear force deformation curves of beam-column joint in structural frame composed of steel beams and reinforced concrete columns. *Journal of Structure and Construction Engineering*, **429**, 55-64. (in Japanese)

[4] Sakaguchi N, Architectural Institute of Japan (1992): Stiffness, strength and deformation of frames composed of reinforced concrete columns and steel beams. *Journal of Structure and Construction Engineering*, **437**, 125-134. (in Japanese)

